

Precision Calculation of $np \rightarrow d\gamma$ Cross Section for Big-Bang Nucleosynthesis

Gautam Rupak
Department of Physics,
University of Washington,
Seattle, WA 98195

Abstract

An effective field theory calculation of the $np \rightarrow d\gamma$ cross section accurate to 1% for center of mass energies $E \lesssim 1$ MeV is presented. At these energies, which are relevant for big-bang nucleosynthesis, isovector magnetic transitions $M1_V$ and isovector electric transitions $E1_V$ give the dominant contributions. The $M1_V$ amplitude is calculated up to next-to-next-to-leading order (N²LO), and the contribution from the associated four-nucleon-one-photon operator is determined from the cold neutron capture rate. The $E1_V$ amplitude is calculated up to N⁴LO. The four-nucleon-one-photon operator contribution to $E1_V$ is determined from the related deuteron photodisintegration reaction $\gamma d \rightarrow np$.

September 1999

I. INTRODUCTION

Big-bang nucleosynthesis (BBN) is a cornerstone of big-bang cosmology [1]. Primordial deuterium production is very sensitive to the baryon density of the universe and thus the BBN prediction of deuterium abundance can be used to infer this baryon density. These deuterium abundance calculations use the cross section for $np \rightarrow d\gamma$ as one of the inputs. Thus, an accurate estimation of the $np \rightarrow d\gamma$ cross section is essential to the BBN prediction of deuterium and other light element abundances. At the energies relevant for BBN, $0.02 \lesssim E \lesssim 0.2$ MeV, this reaction is not well-measured experimentally and there are significant theoretical uncertainties [1]. For example, in the model calculation of Smith, Kawano and Malaney (SKM) an error of 5% was assigned to the cross section for $np \rightarrow d\gamma$ [2]. The SKM result agrees with a slightly earlier evaluation from ENDF/B-VI [3]. The errors in this calculation are not well documented and they could be as large as 10-15% [4]. There is a much earlier calculation (1967) by Fowler, Caughlan and Zimmerman [5] which agrees with the SKM and ENDF/B-VI result for energies $E \lesssim 0.1$ MeV but disagrees significantly at higher energies [2]. A recent model independent calculation by Chen and Savage, using a low energy effective field theory (EFT) predicted a theoretical uncertainty of 4% [6]. This work is a one higher order calculation in the perturbative expansion of the EFT used in Ref. [6]. The theoretical uncertainty is estimated to be $\lesssim 1\%$ for center of mass energies $E \lesssim 1$ MeV.

For thermal neutrons ($E \sim 10^{-8}$ MeV), the cross section for $np \rightarrow d\gamma$ is dominated by the isovector magnetic transition $M1_V$ from the 1S_0 isovector channel to the 3S_1 isoscalar channel. At higher energies, $E \sim 1$ MeV, the cross section for $np \rightarrow d\gamma$ is dominated by isovector electric transitions $E1_V$ from the isovector P -wave to 3S_1 channel. At the energies relevant for BBN, the $M1_V$ and $E1_V$ transitions give comparable contributions.

Effective field theory is a useful tool in the study of physical processes with a clear separation of scales. This is the case for the reaction $np \rightarrow d\gamma$. At energies relevant for BBN, the nucleon center of mass momentum $p \sim 30$ MeV, the deuteron binding momentum $\gamma_t \sim 45$ MeV and the inverse of the singlet channel 1S_0 neutron-proton scattering length $1/a^{exp} \sim 8$ MeV are all much smaller than the mass of the lightest meson, the pion with mass $m_\pi \sim 140$ MeV. Thus a low energy EFT can be constructed for momenta much below the pion mass m_π , by integrating out the pions and other heavier degrees of freedom from the theory. The strong interaction of the nucleons is then described by four-nucleon local operators [7,8]. The effects of the particles that were integrated out of the theory are encoded in a perturbative expansion of local operators, where the expansion parameter is expected to be Q/m_π with $p, \gamma_t, 1/a^{exp} \sim Q$. The perturbative description of the low energy physics then allows a systematic estimation of errors at any order in the perturbation.

Recently there has been much discussion [6–9] about the role EFT can play in improving the ‘traditional’ results obtained using effective-range theory (ERT) for low energy observables in the two nucleon system. It was shown in Ref. [10] that for nucleon-nucleon scattering, ERT and low energy EFT are equivalent. In some processes, however, involving external currents, e.g. electron-deuteron scattering, the ERT amplitude differs from the EFT result due to the absence of two-body current operators. The most general set of allowed multi-nucleon-external-field operators contains operators that need not be related to the nucleon-nucleon scattering operators, included in ERT, by gauging the derivatives through

minimal photon coupling. Including multi-nucleon-external-field operators, e.g. two-body currents, is straightforward in EFT. The deviation of the ERT result from EFT due to the absence of certain two-body current operators will be greater if these operators appear at lower order in the perturbative EFT expansion. For example, in the EFT without dynamical pions a four-nucleon-one-photon operator contributes to deuteron quadrupole moment μ_Q at next-to-leading order (NLO) [8]. The absence of such an operator in the ERT could be responsible for potential models' under prediction of μ_Q by about 5% [8,11] in the impulse approximation (IA) [12,13]. In $np \rightarrow d\gamma$, the $M1_V$ transition amplitude also involves a four-nucleon-one-photon operator at NLO in the EFT that is not included in the ERT. This operator contributes about 5% to the cold neutron capture cross section $\sigma^{exp} = 334.2$ mb and about 2% at energy $E \sim 0.5$ MeV ¹. On the other hand, the $E1_V$ amplitude can be written entirely in terms of nucleon-nucleon scattering operators up to N³LO and reduces to the ERT result at this order.

The $M1_V$ transition amplitude has been calculated up to NLO [6,15,16]. The unknown coupling L_1^{M1} , associated with a four-nucleon-one-photon operator, appearing at this order can be determined from the cold neutron capture rate of $\sigma^{exp} = 334.2 \pm 0.5$ mb [17] at incident neutron speed $v = 2200$ m/s. The $E1_V$ transition amplitude has been calculated up to N³LO [6]. In this work, we calculate the $M1_V$ transition amplitude up to N²LO and the $E1_V$ transition amplitude up to N⁴LO. For the $M1_V$ amplitude, there is a new unknown coupling $L_3^{M1_V}$ at N²LO. Only a linear combination of $L_1^{M1_V}$ and $L_3^{M1_V}$ contributes at very low momentum. We derive perturbative constraints [16,18] on these couplings to reproduce the low energy cross section σ^{exp} . For the $E1_V$ transition, there is a coupling $L_1^{E1_V}$ at N⁴LO that is not determined from nucleon-nucleon scattering data. We determine L_1^{E1} from a χ^2 fit to data [19] for the related process of deuteron photodisintegration $\gamma d \rightarrow np$.

The organization of the paper is as follows: We first describe the relevant Lagrangian and the power counting rules in Section II. This section is rather technical and primarily used to define various parameters that enter the expression for the cross section. The calculation of the total cross section is presented in Subsections III A, III B and III C. The renormalization group (RG) flow of the couplings is discussed in some detail, and from the analysis, constraints on some of the couplings are derived. In Subsection III D, all the remaining couplings are determined. In Section IV, we tabulate the calculated cross section for some energies relevant for BBN, discuss the theoretical errors, and compare our results with the corresponding values from the on-line ENDF/B-VI database [3]. Summary and conclusions follow in Section V.

¹We would like to mention that for thermal neutrons, meson exchange currents explain the 10% discrepancy in the cross section for $np \rightarrow d\gamma$ between potential models in IA and σ^{exp} [14]. However, modern potential models, e.g. Argonne v_{18} , with meson exchange currents and relativistic corrections underpredict μ_Q by about 4% [13].

II. THE LAGRANGIAN AND POWER COUNTING

A perturbative EFT calculation requires a Lagrangian, and a set of power counting rules that determine the relative sizes of diagrams contributing to a physical process. The nucleon kinetic energy term is

$$\mathcal{L}_1 = N^\dagger \left[iD_0 + \frac{\mathbf{D}^2}{2M_N} - \frac{D_0^2}{2M_N} \right] N, \quad (2.1)$$

where the covariant derivative is

$$D^\mu = \partial^\mu + ie \frac{1 + \tau_3}{2} A^\mu. \quad (2.2)$$

N is an isodoublet field representing the nucleons, the matrix τ_3 acts on the nucleon isospin space and $M_N = 938.92$ MeV is the isospin averaged value of the nucleon mass. Note that the D_0^2 term in Eq. (2.1) includes all the relativistic corrections to the nucleon kinetic energy [8].

The two-body Lagrangian relevant for radiative capture process $np \rightarrow d\gamma$ and the photo-disintegration of the deuteron $\gamma d \rightarrow np$ can be divided into (a) a Lagrangian \mathcal{L}_2^S contributing to nucleon-nucleon scattering in the 3S_1 and 1S_0 channels, (b) a Lagrangian \mathcal{L}_2^P contributing to nucleon-nucleon scattering in relative angular momentum states 3P_0 , 3P_1 , 3P_2 and (c) a Lagrangian \mathcal{L}_2^{EM} describing two-body currents that are not contained in the previous two Lagrangians.

A. Lagrangian for S -State Nucleon-Nucleon Interaction: \mathcal{L}_2^S

We start by describing the Lagrangian contributing to the final or initial state nucleon-nucleon interaction responsible for binding the deuteron. In the 3S_1 channel, up to N⁴LO:

$$\begin{aligned} \mathcal{L}_2^{(^3S_1)} = & -C_0(N^T P_i N)^\dagger (N^T P_i N) + \frac{C_2}{2} \left[(N^T \mathcal{O}_i^{(2)} N)^\dagger (N^T P_i N) + h.c. \right] \\ & -C_4(N^T \mathcal{O}_i^{(2)} N)^\dagger (N^T \mathcal{O}_i^{(2)} N) - \frac{\tilde{C}_4}{2} \left[(N^T \mathcal{O}_i^{(4)} N)^\dagger (N^T P_i N) + h.c. \right] \\ & + \frac{C_6}{2} \left[(N^T \mathcal{O}_i^{(4)} N)^\dagger (N^T \mathcal{O}_i^{(2)} N) + h.c. \right] + \frac{\tilde{C}_6}{2} \left[(N^T \mathcal{O}_i^{(6)} N)^\dagger (N^T P_i N) + h.c. \right] \\ & -C_8^\alpha (N^T \mathcal{O}_i^{(4)} N)^\dagger (N^T \mathcal{O}_i^{(4)} N) - \frac{C_8^\beta}{2} \left[(N^T \mathcal{O}_i^{(6)} N)^\dagger (N^T \mathcal{O}_i^{(2)} N) + h.c. \right] \\ & + C_2^{(sd)} \left[(N^T P_i N)^\dagger (N^T \mathcal{O}^{xyj} N) \mathcal{T}^{ijxy} + h.c. \right], \end{aligned} \quad (2.3)$$

where summation over the repeated indices is implied. The P_i matrices are used to project onto the 3S_1 state,

$$P_i \equiv \frac{1}{\sqrt{8}} \sigma_2 \sigma_i \otimes \tau_2, \quad \text{Tr}[P_i^\dagger P_j] = \frac{1}{2} \delta_{ij}, \quad (2.4)$$

where the σ matrices act on the nucleon spin space and the τ matrices act on the nucleon isospin space. The Galilean invariant covariant derivative operators are defined as:

$$\begin{aligned}
\mathcal{O}_i^{(2)} &= \frac{1}{4} \left[\overleftarrow{\mathbf{D}}^2 P_i - 2 \overleftarrow{\mathbf{D}} P_i \overrightarrow{\mathbf{D}} + P_i \overrightarrow{\mathbf{D}}^2 \right] \\
\mathcal{O}_i^{(4)} &= \frac{1}{16} \left[\overleftarrow{\mathbf{D}}^4 P_i - 4 \overleftarrow{\mathbf{D}}^3 P_i \overrightarrow{\mathbf{D}} + 6 \overleftarrow{\mathbf{D}}^2 P_i \overrightarrow{\mathbf{D}}^2 - 4 \overleftarrow{\mathbf{D}} P_i \overrightarrow{\mathbf{D}}^3 + P_i \overrightarrow{\mathbf{D}}^4 \right] \\
\mathcal{O}_i^{(6)} &= \frac{1}{64} \left[\overleftarrow{\mathbf{D}}^6 P_i - 6 \overleftarrow{\mathbf{D}}^5 P_i \overrightarrow{\mathbf{D}} + 15 \overleftarrow{\mathbf{D}}^4 P_i \overrightarrow{\mathbf{D}}^2 - 20 \overleftarrow{\mathbf{D}}^3 P_i \overrightarrow{\mathbf{D}}^3 \right. \\
&\quad \left. + 15 \overleftarrow{\mathbf{D}}^2 P_i \overrightarrow{\mathbf{D}}^4 - 6 \overleftarrow{\mathbf{D}} P_i \overrightarrow{\mathbf{D}}^5 + P_i \overrightarrow{\mathbf{D}}^6 \right] \\
\mathcal{O}^{xyj} &= \frac{1}{4} \left[\overleftarrow{\mathbf{D}}^x \overleftarrow{\mathbf{D}}^y P_j - \overleftarrow{\mathbf{D}}^x P_j \overrightarrow{\mathbf{D}}^y - \overleftarrow{\mathbf{D}}^y P_j \overrightarrow{\mathbf{D}}^x + P_j \overrightarrow{\mathbf{D}}^x \overrightarrow{\mathbf{D}}^y \right] \\
\mathcal{T}^{ijxy} &= \left(\delta^{ix} \delta^{jy} - \frac{1}{n-1} \delta^{ij} \delta^{xy} \right),
\end{aligned} \tag{2.5}$$

where n is the number of space-time dimensions. For the $M1_V$ transition there is also initial or final state nucleon-nucleon interaction in the 1S_0 channel and the Lagrangian has the same form as the one described in Eq. (2.3), with the corresponding projections onto the 1S_0 channel. Note that there is no corresponding S - D mixing term, $C_2^{(sd)}$, in the 1S_0 channel.

In 1997, Kaplan, Savage and Wise (KSW) formulated a systematic power counting for calculating the cross sections of two-nucleon processes in the context of EFT [7]. One key ingredient in the KSW scheme is the non-perturbative treatment of the large S -channel nucleon-nucleon scattering length. KSW power counting can be implemented using power divergence subtraction (PDS) where one subtracts the loop-divergences in both $n = 3$ and $n = 4$ space-time dimensions. An alternative to PDS is off-shell subtraction, where the divergences are regulated by subtracting the amplitude at an off-shell momentum point [20]. In this paper, we will use PDS scheme.

The KSW power counting is as follows: The expansion parameter is Q/Λ . The nucleon center of mass momentum p , the deuteron binding momentum γ_t , the inverse of the 1S_0 channel scattering length $1/a^{exp}$ and the renormalization scale μ are formally considered $\mathcal{O}(Q)$ and $\Lambda \sim m_\pi/2$ for this low energy EFT (the factor of half comes from the analytic structure of the one-pion-exchange contributions). The couplings C_{2n} scale as $1/Q^{n+1}$, \tilde{C}_{2n} scale as $1/Q^n$ and $C_2^{(sd)}$ scales as $1/Q$. For the low energy theory, we formally take $m_\pi/M_N \sim Q/\Lambda$. Thus, relativistic corrections which come in as p^2/M_N^2 , $\gamma_t^2/M_N^2 \sim Q^2/M_N^2 = Q^2/m_\pi^2 \times m_\pi^2/M_N^2$ contribute at N⁴LO.

It is a feature of the KSW power counting that the EFT couplings associated with S -state interactions scale with some powers of Q . This is because the couplings are fine-tuned to reproduce the large scattering lengths that one sees in the 1S_0 and 3S_1 channels. In order to reproduce the exact deuteron pole, the coefficients C_{2n} are expanded in powers of Q :

$$\begin{aligned}
C_0 &= C_{0,-1} + C_{0,0} + \cdots \\
C_2 &= C_{2,-2} + C_{2,-1} + \cdots \\
&\vdots
\end{aligned} \tag{2.6}$$

where the second subscript denotes the Q scaling. The EFT couplings C_{2n} are determined by matching the nucleon-nucleon scattering amplitude calculated in EFT [7,8,18] and that obtained from the ERE [21]:

$$p \cot \delta = -\gamma_t + \frac{1}{2}\rho_d (p^2 + \gamma_t^2) + \frac{1}{2}w_2 (p^2 + \gamma_t^2)^2 + \dots \quad (2.7)$$

To the order we are working, the deuteron binding momentum $\gamma_t \approx \gamma - \gamma^3/(8M_N^2)$, where $\gamma = \sqrt{M_N B}$, and $B = 2.2246$ MeV [22] is the deuteron binding energy. The coupling $C_2^{(sd)} = 3\eta_d/(\sqrt{2}\gamma^2)$ is determined from the S - D mixing parameter $\bar{\epsilon}_1$ [8,16,23], where $\eta_d = 0.02534$ is the D -wave to S -wave ratio at the deuteron pole [22]. Notice that $C_2^{(sd)}$ is smaller than naive power counting estimate because of the smallness of the parameter η_d .

For our calculation, we need the 3S_1 channel initial or final state interaction up to N⁴LO and the 1S_0 interaction up to N²LO. In the 3S_1 channel, at N⁴LO only four experimental inputs (γ , ρ_d , w_2 and η_d) enter the scattering amplitude. The EFT couplings that depend on the high energy scale can all be expressed in terms of these four parameters. However, only the combinations $C_4 + \tilde{C}_4$ and $C_8^\alpha + C_8^\beta \equiv C_8$ contribute to nucleon-nucleon scattering and so nucleon-nucleon scattering data cannot be used to separate C_4 from \tilde{C}_4 , and C_8^α from C_8^β . We use the effective range $\rho_d = 1.764$ fm and shape parameter $w_2 = 0.778$ fm³ [22]. In the 1S_0 channel, at N²LO the nucleon-nucleon scattering amplitude is completely determined by the scattering length a^{exp} and the effective range r_0 . The EFT couplings C_{2n} are determined in terms of these two parameters. Note that the experimentally measured scattering length a^{exp} , for neutron-proton scattering in the singlet channel 1S_0 , gets about a 3% contribution from magnetic moment interaction [13]. Isospin-breaking single magnetic photon exchange gives the dominant correction and it is described by the Lagrangian

$$\mathcal{L} = \frac{e\kappa_1}{2M_N} N^\dagger \tau_3 \sigma \cdot \mathbf{B} N, \quad (2.8)$$

where \mathbf{B} is the magnetic field and $\kappa_1 = 2.353$ is the isovector nucleon magnetic moment in nuclear magnetons. These N²LO interactions must be included in the $M1_V$ amplitude. We implicitly include the magnetic moment interactions by using the experimental value $a^{exp} = -23.75$ fm [24]. For the effective range we take $r_0 = 2.73$ fm.

B. Lagrangian for P -State Nucleon-Nucleon Interaction: \mathcal{L}_2^P

In this subsection, the second Lagrangian \mathcal{L}_2^P is described. For the $E1_V$ transition amplitude, there are also initial or final state nucleon-nucleon interactions in relative angular momentum states 3P_0 , 3P_1 , 3P_2 described by the Lagrangian [6]:

$$\begin{aligned} \mathcal{L}_2^P = & \left(C_2^{(3P_0)} \delta_{xy} \delta_{wz} + C_2^{(3P_1)} [\delta_{xw} \delta_{yz} - \delta_{xz} \delta_{yw}] + C_2^{(3P_2)} \left[2\delta_{xw} \delta_{yz} + 2\delta_{xz} \delta_{yw} - \frac{4}{3} \delta_{xy} \delta_{wz} \right] \right) \\ & \times \frac{1}{4} (N^T \mathcal{O}_{xy}^{(1,P)} N)^\dagger (N^T \mathcal{O}_{wz}^{(1,P)} N), \end{aligned} \quad (2.9)$$

where the P -wave operator is

$$\mathcal{O}_{ij}^{(1,P)} = \overleftarrow{\mathbf{D}}_i P_j^{(P)} - P_j^{(P)} \overrightarrow{\mathbf{D}}_i, \quad (2.10)$$

and $P_i^{(P)}$ are the spin-isospin projectors for the isotriplet, spintriplet channel

$$P_i^{(P)} \equiv \frac{1}{\sqrt{8}} \sigma_2 \sigma_i \tau_2 \tau_3, \quad \text{Tr} [P_i^{(P)} P_j^{(P)}] = \frac{1}{2} \delta_{ij}. \quad (2.11)$$

The power counting of the P -state couplings is straightforward. Since there are no fine tuned high energy scales in the P -state scattering, the couplings that are dependent only on the high energy physics are $\mathcal{O}(1)$ i.e. they do not scale with Q . As a result, the next set of P -state operators, suppressed by two extra powers of momentum p , enters only at N⁵LO. Only the linear combination

$$C_p \equiv C_2^{(3P_0)} + 2C_2^{(3P_1)} + \frac{20}{3}C_2^{(3P_2)} \quad (2.12)$$

enters our calculation and Nijmegen phase shift analysis [12,25] fixes $C_p = -1.49 \text{ fm}^4$ [6].

C. Lagrangian for Two-Body Currents: \mathcal{L}_2^{EM}

Finally, we discuss the two-body currents contributing to $np \rightarrow d\gamma$ or $\gamma d \rightarrow np$, which are not included in the previous two Lagrangians \mathcal{L}_2^S and \mathcal{L}_2^P . These operators are not related by gauge transformation to the nucleon-nucleon scattering operators in \mathcal{L}_2^S and \mathcal{L}_2^P .

$$\begin{aligned} \mathcal{L}_2^{EM} = & e L_1^{M1V} (N^T P_i N)^\dagger (N^T \bar{P}_3 N) \mathbf{B}_i - e L_3^{M1V} (N^T \mathcal{O}_i^{(2)} N)^\dagger (N^T \bar{P}_3 N) \mathbf{B}_i \\ & - e \tilde{L}_3^{M1V} (N^T P_i N)^\dagger (N^T \bar{\mathcal{O}}_3^{(2)} N) \mathbf{B}_i + \frac{1}{2} e L_1^{E1V} (N^T \mathcal{O}_{ia}^{(1,P)} N)^\dagger (N^T P_a N) \mathbf{E}_i \\ & - \frac{1}{2} e L_3^{E1V} (N^T \mathcal{O}_{ia}^{(1,P)} N)^\dagger (N^T \mathcal{O}_a^{(2)} N) \mathbf{E}_i - \frac{1}{2} e \tilde{L}_3^{E1V} (N^T \mathcal{O}_{ia}^{(3,P)} N)^\dagger (N^T P_a N) \mathbf{E}_i \\ & + \frac{1}{2} e L_5^{E1V} (N^T \mathcal{O}_{ia}^{(1,P)} N)^\dagger (N^T \mathcal{O}_a^{(4)} N) \mathbf{E}_i + \frac{1}{2} e \tilde{L}_5^{E1V} (N^T \mathcal{O}_{ia}^{(3,P)} N)^\dagger (N^T \mathcal{O}_a^{(2)} N) \mathbf{E}_i \\ & - e L_2^{M1S} i \epsilon_{ijk} (N^T P_i N)^\dagger (N^T P_j N) \mathbf{B}_k + h.c., \end{aligned} \quad (2.13)$$

where \mathbf{E} and \mathbf{B} are the electric and magnetic fields respectively, and

$$\begin{aligned} \bar{P}_i &= \frac{1}{\sqrt{8}} \sigma_2 \otimes \tau_2 \tau_i \\ \bar{\mathcal{O}}_i^{(2)} &= \frac{1}{4} \left[\overleftarrow{\mathbf{D}}^2 \bar{P}_i - 2 \overleftarrow{\mathbf{D}} \bar{P}_i \overrightarrow{\mathbf{D}} + \bar{P}_i \overrightarrow{\mathbf{D}}^2 \right] \\ \mathcal{O}_{ij}^{(3,P)} &= \frac{1}{4} \left[\overleftarrow{\mathbf{D}}_i \overleftarrow{\mathbf{D}}^2 P_j^{(P)} - 2 \overleftarrow{\mathbf{D}}_i \overleftarrow{\mathbf{D}}_k P_j^{(P)} \overrightarrow{\mathbf{D}}_k + \overleftarrow{\mathbf{D}}_i P_j^{(P)} \overrightarrow{\mathbf{D}}^2 \right. \\ &\quad \left. - \overleftarrow{\mathbf{D}}^2 P_j^{(P)} \overrightarrow{\mathbf{D}}_i + 2 \overleftarrow{\mathbf{D}}_k P_j^{(P)} \overrightarrow{\mathbf{D}}_k \overleftarrow{\mathbf{D}}_i - P_j^{(P)} \overrightarrow{\mathbf{D}}^2 \overrightarrow{\mathbf{D}}_i \right]. \end{aligned} \quad (2.14)$$

The superscript on the two-body current couplings L 's denote the transitions that the particular operators contribute to. For the $M1_V$ transition only a specific p independent combination of L_1^{M1V} and L_3^{M1V} contributes and we fix it from the cold neutron capture rate $np \rightarrow d\gamma$. Renormalization group (RG) flow analysis determines \tilde{L}_3^{M1V} in terms L_1^{M1V} , $C_2^{(1S_0)}$ and $C_2^{(3S_0)}$. For the $E1_V$ transition, only a combination, L_{E1} , of L_1^{E1V} , L_3^{E1V} and L_5^{E1V} enters the calculation at N⁴LO and it is fixed from a χ^2 fit to the related deuteron breakup process $\gamma d \rightarrow np$ [6]. The other operators contribute at orders higher than considered here. The

RG analysis of these operators is discussed in more detail below, in Subsections III A, III B. Finally, the observed value of the deuteron magnetic moment μ_M fixes the isoscalar magnetic moment coupling $L_2^{(M1S)} = -0.149 \text{ fm}^4$ [8,26].

In the last three subsections, we described the Lagrangian and the power counting rules relevant to our calculation. Now, the calculation for the total cross section is presented, along with the estimated theoretical uncertainty. This is followed by the discussion of a matching procedure for determining the unknown couplings L_1^{M1V} and L_3^{M1V} . The parameter L_{E1} is fixed from the $\gamma d \rightarrow np$ data.

III. CALCULATION AND ANALYSIS

The amplitude Γ for low energy $np \rightarrow d\gamma$ reaction is [15,16]:

$$\begin{aligned} i \Gamma = & e X_{E1V} U^T \tau_2 \tau_3 \sigma_2 \sigma \cdot \epsilon_{(d)}^* U p \cdot \epsilon_{(\gamma)}^* + ie X_{M1V} \varepsilon^{abc} \epsilon_{(d)}^{*a} \mathbf{k}^b \epsilon_{(\gamma)}^{*c} U^T \tau_2 \tau_3 \sigma_2 U \\ & + e X_{M1S} \frac{1}{\sqrt{2}} U^T \tau_2 \sigma_2 \left[\sigma \cdot \mathbf{k} \epsilon_{(d)}^* \cdot \epsilon_{(\gamma)}^* - \epsilon_{(d)}^* \cdot \mathbf{k} \epsilon_{(\gamma)}^* \cdot \sigma \right] U \\ & + e X_{E2S} \frac{1}{\sqrt{2}} U^T \tau_2 \sigma_2 \left[\sigma \cdot \mathbf{k} \epsilon_{(d)}^* \cdot \epsilon_{(\gamma)}^* + \epsilon_{(d)}^* \cdot \mathbf{k} \epsilon_{(\gamma)}^* \cdot \sigma - \frac{2}{n-1} \sigma \cdot \epsilon_{(d)}^* \mathbf{k} \cdot \epsilon_{(\gamma)}^* \right] U, \end{aligned} \quad (3.1)$$

where only the lowest partial waves are shown: isovector electric dipole capture of nucleons in a P -wave with amplitude X_{E1V} , isovector magnetic dipole capture of nucleons in 1S_0 state with amplitude X_{M1V} , isoscalar magnetic dipole capture of nucleons in 3S_1 state with amplitude X_{M1S} and isoscalar electric quadrupole capture of nucleons with amplitude X_{E2S} . We use dimensional regularization to regulate divergences and n represents the number of space-time dimensions. The U 's are two component nucleon spinor wave functions. $|\mathbf{p}| \equiv p$ is the nucleon center of mass momentum, k is the outgoing photon momentum, and $\epsilon_{(\gamma)}$ and $\epsilon_{(d)}$ are the photon and deuteron polarization vectors respectively. The following dimensionless amplitudes, \tilde{X} , are defined

$$\begin{aligned} \frac{|\mathbf{p}| M_N}{\gamma^2 + p^2} X_{E1V} &= i \frac{2}{M_N} \sqrt{\frac{\pi}{\gamma^3}} \tilde{X}_{E1V}, & X_{M1V} &= i \frac{2}{M_N} \sqrt{\frac{\pi}{\gamma^3}} \tilde{X}_{M1V} \\ X_{M1S} &= i \frac{2}{M_N} \sqrt{\frac{\pi}{\gamma^3}} \tilde{X}_{M1S}, & X_{E2S} &= i \frac{2}{M_N} \sqrt{\frac{\pi}{\gamma^3}} \tilde{X}_{E2S}, \end{aligned} \quad (3.2)$$

and the total cross section for $np \rightarrow d\gamma$ is then written as:

$$\begin{aligned} \sigma &= 4\alpha\pi \left(1 - \frac{2p^4 + 4p^2\gamma^2 + 3\gamma^4}{4M_N^2(p^2 + \gamma^2)} \right) \frac{(\gamma^2 + p^2)^3}{\gamma^3 M_N^4 p} \frac{1}{2} \int_{-1}^1 d\cos\theta \left[\frac{3}{2} |\tilde{X}_{E1V}|^2 \sin^2\theta + |\tilde{X}_{M1V}|^2 \right. \\ &\quad \left. + |\tilde{X}_{M1S}|^2 + |\tilde{X}_{E2S}|^2 \right] \\ &\equiv 4\alpha\pi \left(1 - \frac{2p^4 + 4p^2\gamma^2 + 3\gamma^4}{4M_N^2(p^2 + \gamma^2)} \right) \frac{(\gamma^2 + p^2)^3}{\gamma^3 M_N^4 p} \left[\langle \tilde{X}_{E1V} \rangle^2 + \langle \tilde{X}_{M1V} \rangle^2 + \langle \tilde{X}_{M1S} \rangle^2 + \langle \tilde{X}_{E2S} \rangle^2 \right], \end{aligned} \quad (3.3)$$

where the deuteron mass is $M_d \approx 2M_N - \gamma^2/M_N$ [8]. The relativistic corrections enter at N⁴LO and so only the $E1V$ cross section which is calculated to this order receives such contributions.

A. Isovector Electric Transition: $E1_V$

The $E1_V$ amplitude up to N⁴LO is

$$\begin{aligned} \tilde{X}_{E1_V} = & -\frac{M_N p \gamma^2}{(p^2 + \gamma^2)^2} \left[1 + \frac{\rho_d \gamma}{2} + \frac{3}{8} \rho_d^2 \gamma^2 + \frac{5}{16} \rho_d^3 \gamma^3 + \frac{35}{128} \rho_d^4 \gamma^4 - \frac{5}{2} \eta_d^2 + \frac{(p^2 + \gamma^2)^2}{2M_N} L_{E1} \right. \\ & + \frac{M_N \gamma}{12\pi} \left(\frac{\gamma^2}{3} + p^2 \right) C_p \left(1 + \frac{\rho_d \gamma}{2} \right) + \frac{|p|}{M_N} \cos \theta \left(1 + \frac{\rho_d \gamma}{2} + \frac{3}{8} \rho_d^2 \gamma^2 \right) \\ & \left. + \frac{p^2}{M_N^2} \cos^2 \theta - \frac{8p^4 + 17p^2 \gamma^2 + 5\gamma^4}{16M_N^2(p^2 + \gamma^2)} \right], \end{aligned} \quad (3.4)$$

where the relativistic corrections contribute at N⁴LO as they are suppressed by additional powers of $(m_\pi/M_N)^2$, and

$$\begin{aligned} L_{E1} & \equiv \frac{L_{1,-1}^{E1} - \gamma^2 L_{3,-3}^{E1} + \gamma^4 L_{5,-5}^{E1} + \gamma^4 M_N (C_{8,-5}^\beta + 2C_{8,-5}^{(3S_1)}) - M_N \eta \tilde{C}_{4,-1}}{C_{0,-1}^{(3S_1)}} \quad (3.5) \\ \eta \tilde{C}_{4,-1} & \equiv \tilde{C}_{4,-1}^{(3S_1)} + \frac{2\pi}{M_N} \frac{\rho_d w_2 \gamma^2}{(\mu - \gamma)^3}. \end{aligned}$$

The $\eta \tilde{C}_{4,-1}$ coupling renormalizes contributions proportional to η_d^2 in Eq. (3.4). The renormalization scale μ independent parameter $L_{E1} \sim \mathcal{O}(1)$ can be simplified further. We assume that all the couplings have a sensible large scattering length ($\gamma \rightarrow 0$) limit. Then it follows that at the high scale $\mu = \Lambda$, only the combination $(L_{1,-1}^{E1} - M_N \eta \tilde{C}_{4,-1})/C_{0,-1}^{(3S_1)}$ contributes a $\mathcal{O}(1)$ term. The other combinations, e.g. $\gamma^2 L_{3,-3}^{E1}/C_{0,-1}^{(3S_1)}$, contribute terms of $\mathcal{O}(Q^2)$ and higher. Thus RG analysis gives

$$L_{E1} \equiv \frac{L_{1,-1}^{E1} - M_N \eta \tilde{C}_{4,-1}}{C_{0,-1}^{(3S_1)}} (1 + \mathcal{O}(Q^2)), \quad (3.6)$$

and we keep only the leading contribution to L_{E1} for our calculation. It is possible to make an order of magnitude estimate for L_{E1} . The contribution from S - D mixing, proportional to η_d^2 , is numerically negligible at N⁴LO even though it is formally a N⁴LO term. Thus, ignoring contribution from $\eta \tilde{C}_{4,-1}$, we estimate at the renormalization scale $\mu = \Lambda \sim m_\pi/2$:

$$\begin{aligned} |C_{0,-1}^{(3S_1)}| & \sim \frac{4\pi}{M_N} \frac{1}{\Lambda}, & |L_{1,-1}^{E1}| & \sim \frac{1}{M_N \Lambda^4} \\ \Rightarrow |L_{E1}| & \sim 2 \text{ fm}^3, \end{aligned} \quad (3.7)$$

where factors of $1/M_N$ from the nucleon loops were included.

In Eq. (3.4), we have only kept the terms that contribute to the total cross section after summing over deuteron, photon and nucleon polarizations. We have included the formally N²LO contribution proportional to $\cos \theta$. This term, odd in $\cos \theta$, contributes to the cross section only at N⁴LO after the integration over the angle θ , Eq. (3.3). In obtaining Eq. (3.4), we have also used the fact that only the μ independent combination

$$\frac{\tilde{L}_{3,-3}^{(E1_V)} - \gamma^2 \tilde{L}_{5,-5}^{(E1_V)} - 2M_N \tilde{C}_{6,-3}^{(^3S_1)} + 2M_N \gamma^2 C_{8,-5}^\beta}{C_{0,-1}^{(^3S_1)}} \quad (3.8)$$

enters our result. From RG analysis, by flowing the couplings to the high scale $\mu = \Lambda$, we see that the numerator is $\mathcal{O}(1/Q)$ instead of the naive counting of $1/Q^3$. Thus this particular combination of operators contributes starting at N⁶LO and we ignore it in this N⁴LO calculation.

The dominant contribution beyond leading order, Eq. (3.4), is a simple expansion of the factor $\sqrt{Z_d} \equiv 1/\sqrt{1 - \rho_d \gamma}$ from the deuteron wave function renormalization

$$\mathcal{Z} = -\frac{8\pi\gamma}{M_N^2} \left[1 + \rho_d \gamma + \rho_d^2 \gamma^2 + \rho_d^3 \gamma^3 + \rho_d^4 \gamma^4 + \eta_d^2 \frac{7\gamma - 5\mu}{\mu - \gamma} + \frac{\gamma^2}{8M_N^2} \frac{7\mu - 5\gamma}{\mu - \gamma} + \dots \right]. \quad (3.9)$$

In Eq. (3.9), the $\rho_d \gamma$ terms inside the square brackets are from the expansion of Z_d , and the sixth and seventh terms arise from the S - D mixing and relativistic corrections to the deuteron two-point function respectively.

Amplitudes for inelastic processes, e.g. $E1_V$ and $M1_V$ transitions, with a deuteron in the final state involve a factor of $\sqrt{Z_d}$. On the other hand amplitudes for elastic processes involving a deuteron, e.g. the deuteron quadrupole form factor F_Q , include a factor of Z_d . In Ref. [9], an expansion in $Z_d - 1$ was proposed which resums the expansion in $\rho_d \gamma$ seen in Eq. (3.9) and thereby reproduces the exact factor of Z_d at NLO for the amplitude for elastic processes. On the other hand, amplitudes involving inelastic processes on the deuteron have this sum incomplete. The factor of $\sqrt{Z_d}$ is reproduced only in perturbation. This incomplete sum can be avoided if we do an expansion in $\sqrt{Z_d} - 1$ to reproduce the exact factor of $\sqrt{Z_d}$ for inelastic processes. The overall factor of Z_d in elastic processes is then reproduced at N²LO instead of NLO. Thus, one might think that the $\sqrt{Z_d} - 1$ expansion is more appropriate to calculate the cross section for the inelastic process $np \rightarrow d\gamma$. However, for the total cross section, which is summed over the nucleon spins and the deuteron and photon polarizations, it is the square of the amplitudes that enter the expression. In such cases it is more convenient to do the expansion in $Z_d - 1$ and reproduce the exact factor of Z_d at NLO. The three different expansions $\rho_d \gamma$, $Z_d - 1$, $\sqrt{Z_d} - 1$ are formally equivalent but correspond to different ways of relating the C_{2n} couplings to the ERE.

In the $Z_d - 1$ expansion, the position of the deuteron pole at momentum $p = i\gamma_t \approx i\gamma$ and the residue Z_d (without S - D mixing) at the pole are used to fix the C_{2n} couplings. One can think of the $Z_d - 1$ expansion as reproducing the asymptotic tail of the deuteron wave function exactly. This allows a better description of data as low energy experiments probe only the large distance behavior of the deuteron wave function. For the rest of the paper we will use the this expansion. The results for \tilde{X} can then be written as:

$$\begin{aligned} \tilde{X}_{E1_V} = & -\frac{M_N p \gamma^2}{(p^2 + \gamma^2)^2} \left[1 + \frac{1}{2}(Z_d - 1) - \frac{1}{8}(Z_d - 1)^2 + \frac{1}{16}(Z_d - 1)^3 - \frac{5}{128}(Z_d - 1)^4 \right. \\ & + \frac{M_N \gamma}{12\pi} \left(\frac{\gamma^2}{3} + p^2 \right) C_p \left(1 + \frac{1}{2}(Z_d - 1) \right) - \frac{5}{2} \eta_d^2 + \frac{(p^2 + \gamma^2)^2}{2M_N} L_{E1} \\ & \left. - \frac{8p^4 + 17p^2 \gamma^2 + 5\gamma^4}{16M_N^2 (p^2 + \gamma^2)} + \frac{|p|}{M_N} \cos \theta \left(1 + \frac{1}{2}(Z_d - 1) - \frac{1}{8}(Z_d - 1)^2 \right) + \frac{p^2}{M_N^2} \cos^2 \theta \right] \end{aligned}$$

$$\langle \tilde{X}_{E1_V} \rangle^2 = \frac{M_N^2 p^2 \gamma^4}{(p^2 + \gamma^2)^4} Z_d \left[1 + \frac{M_N \gamma}{6\pi} \left(\frac{\gamma^2}{3} + p^2 \right) C_p - \frac{5\eta_d^2}{Z_d} + \frac{(p^2 + \gamma^2)^2}{Z_d M_N} L_{E1} \right. \\ \left. - \frac{8p^4 + 17p^2 \gamma^2 + 5\gamma^4}{8Z_d M_N^2 (p^2 + \gamma^2)} + \frac{3}{5} \frac{p^2}{Z_d M_N^2} \right], \quad (3.10)$$

where the last part in $\langle \tilde{X}_{E1_V} \rangle^2$ is from the $\cos^2 \theta$ terms.

The expression for $\langle \tilde{X}_{E1_V} \rangle^2$ in Eq. (3.10) is a perturbative result. There are corrections to this expression from terms that are higher order than the ones considered here in the perturbative expansion. The higher order corrections can be separated into: (a) factors of Z_d from the wavefunction renormalization of the deuteron, Eq. (3.9) and (b) contributions from higher order nucleon-nucleon scattering operators and two-body currents. At $E \sim 1$ MeV, we expect higher order corrections to contribute $(Z_d - 1)(p^2 + \gamma^2)/M_N^2 \sim 0.004$, $5(Z_d - 1)\eta_d^2 \sim 0.002$ due to wave function renormalization. The $Z_d - 1$ corrections to the term involving L_{E1} are renormalized away when we fit L_{E1} . The higher order P -wave operators should contribute $\gamma p^4/(6\pi\Lambda^5)$, $\gamma^3 p^2/(6\pi\Lambda^5)$, $\gamma^5/(6\pi\Lambda^5) \sim 0.01$ with $\Lambda \sim m_\pi/2$. Thus we estimate the theoretical error to be $\sim 1\%$ at energies of $E \sim 1$ MeV. The error is smaller at lower energies.

B. Isovector Magnetic Transition: $M1_V$

A straight forward calculation of $M1_V$ amplitude gives:

$$\begin{aligned} \tilde{X}_{M1_V}^{(0)} &= -\kappa_1 \gamma^2 \left(\frac{1}{p^2 + \gamma^2} - \frac{1}{(\gamma - ip)(\frac{1}{a^{exp}} + ip)} \right) \\ \tilde{X}_{M1_V}^{(1)} &= \frac{1}{2}(Z_d - 1)\tilde{X}_{M1_V}^{(0)} + \kappa_1 \frac{r_0}{2} \frac{p^2 \gamma^2}{(\frac{1}{a^{exp}} + ip)^2 (\gamma - ip)} + \frac{\gamma^2 M_N}{4\pi(\frac{1}{a^{exp}} + ip)} L_{np} \\ \tilde{X}_{M1_V}^{(2)} &= \left(\frac{1}{2}(Z_d - 1) + \frac{r_0}{2} \frac{p^2}{\frac{1}{a^{exp}} + ip} \right) [\tilde{X}_{M1_V}^{(1)} - \frac{1}{2}(Z_d - 1)\tilde{X}_{M1_V}^{(0)}] \\ &\quad - \frac{1}{8}(Z_d - 1)^2 \tilde{X}_{M1_V}^{(0)} + \frac{M_N}{4\pi} \frac{\gamma^2}{\frac{1}{a^{exp}} + ip} \tilde{L}_{np}, \end{aligned} \quad (3.11)$$

where the μ independent parameters are

$$\begin{aligned} L_{np} &\equiv (\mu - \gamma)(\mu - 1/a^{exp}) \left[L_{1,-2}^{M1_V} - \frac{\kappa_1 \pi}{M_N \gamma} \left(\frac{r_0 \gamma}{(\mu - \frac{1}{a^{exp}})^2} + \frac{Z_d - 1}{(\mu - \gamma)^2} \right) \right] \\ \tilde{L}_{np} &\equiv (\mu - \gamma)(\mu - 1/a^{exp}) \left[L_{1,-1}^{M1_V} - \gamma^2 L_{3,-3}^{M1_V} + \frac{\kappa_1 \pi}{M_N \gamma} \frac{(Z_d - 1)^2}{(\mu - \gamma)^2} \right] \\ &= (\mu - \gamma)(\mu - 1/a^{exp}) \left[L_{1,-1}^{M1_V} + \frac{\kappa_1 \pi}{M_N \gamma} \frac{(Z_d - 1)^2}{(\mu - \gamma)^2} \right] (1 + \mathcal{O}(Q^2)). \end{aligned} \quad (3.12)$$

An analysis similar to the one used for L_{E1} , allows us to simplify the parameters L_{np} 's above in Eq. (3.12). A naive estimate gives

$$L_{np} \sim -9 \text{ fm}^2, \quad \tilde{L}_{np} \sim +3 \text{ fm}^2. \quad (3.13)$$

We use the experimentally measured scattering length a^{exp} which includes the effect of single magnetic photon exchange in neutron-proton scattering. In Eq. (3.11), from RG analysis, we used:

$$\tilde{L}_{3,-3}^{M1_V} = \frac{\xi}{(\mu - \gamma)(\mu - \frac{1}{a^{exp}})} - \frac{r_0}{2} \frac{1}{\mu - \frac{1}{a^{exp}}} \left[L_{1,-2}^{M1_V} + \frac{\kappa_1 \pi}{M_N \gamma} \left(\frac{r_0 \gamma}{(\mu - \frac{1}{a^{exp}})^2} - \frac{Z_d - 1}{(\mu - \gamma)^2} \right) \right] . \quad (3.14)$$

The first part $\mathcal{O}(1/Q^2)$ gives higher order corrections to $\tilde{L}_3^{M1_V} \sim 1/Q^3$. So we can set $\xi = 0$ at N⁴LO, and have $\tilde{L}_3^{M1_V}$ completely determined. Up to N²LO

$$|\tilde{X}_{M1_V}|^2 = |\tilde{X}_{M1_V}^{(0)}|^2 + 2Re[\tilde{X}_{M1_V}^{(0)}(\tilde{X}_{M1_V}^{(1)})^*] + |\tilde{X}_{M1_V}^{(1)}|^2 + 2Re[\tilde{X}_{M1_V}^{(0)}(\tilde{X}_{M1_V}^{(2)})^*] . \quad (3.15)$$

The singlet channel scattering length $a^{exp} = -23.75$ fm is unnaturally large and it is easier to do the error analysis for the cross section in the limit $a^{exp} \rightarrow \infty$, with finite corrections from $1/(a^{exp}\gamma)$ and $1/(a^{exp}p)$ terms. There are corrections from initial state interactions in the 1S_0 channel that come in as $r_0^3 p^6 / \gamma^3 \sim 0.03$ at center of mass energy $E = 1$ MeV. There is also a contribution from 1S_0 operators that come in as $r_1 p^4 / \gamma \sim -0.002$, where the shape parameter $r_1 \sim -1$ fm³ is the 1S_0 equivalent of w_2 in Eq. (2.7). The momentum independent corrections from factors of $Z_d - 1$ from deuteron wavefunction renormalization, $r_0 \gamma$ from 1S_0 channel initial state interaction etc. get renormalized away when we fit the parameters L_{np} 's at very low momentum. We estimate the errors in $M1_V$ to be $\sim 3\%$ at $E = 1$ MeV.

C. Isoscalar Magnetic and Electric Transitions: $M1_S$, $E2_S$

The $M1_S$ and $E2_S$ amplitude have been calculated for cold neutron capture [15,16]. The leading contribution from these transitions at non-zero momentum transfer is:

$$\begin{aligned} |\tilde{X}_{M1_S}|^2 &= \frac{M_N^2 \gamma^4}{2\pi^2(p^2 + \gamma^2)} (L_2^{M1_S})^2 (\gamma - \mu)^4 \\ |\tilde{X}_{E2_S}|^2 &= \frac{\gamma^4 \eta_d^2}{100} \frac{(p^4 + 7p^2 \gamma^2 + \gamma^4)}{(p^2 + \gamma^2)^4} . \end{aligned} \quad (3.16)$$

The coupling $L_2^{M1_S}$ can be fitted to the deuteron magnetic moment at the renormalization scale $\mu = m_\pi$ and gives $L_2^{M1_S}(m_\pi) = -0.149$ fm⁴ [8,26].

In the last three subsections, the $np \rightarrow d\gamma$ amplitude in terms of the lowest partial waves, $M1_V$, $E1_V$, $M1_S$ and $E2_S$ has been calculated in terms of three unknown parameters L_{np} , \tilde{L}_{np} and L_{E1} , Eqs. (3.10), (3.11) and (3.16). We now move on to describe how the three unknown parameters L_{np} , \tilde{L}_{np} and L_{E1} can be determined from $np \rightarrow d\gamma$ for cold neutrons and from photodisintegration of the deuteron $\gamma d \rightarrow np$.

D. Determining the Parameters L_{np} , \tilde{L}_{np} and L_{E1}

The leading contributions from each partial wave are shown in Fig. 1. One can see that the $M1_S$ and $E2_S$ transitions can be ignored for a 1% level calculation in the energy range of interest. At center of mass momentum $p_0 = 0.003443$ MeV the cross section for

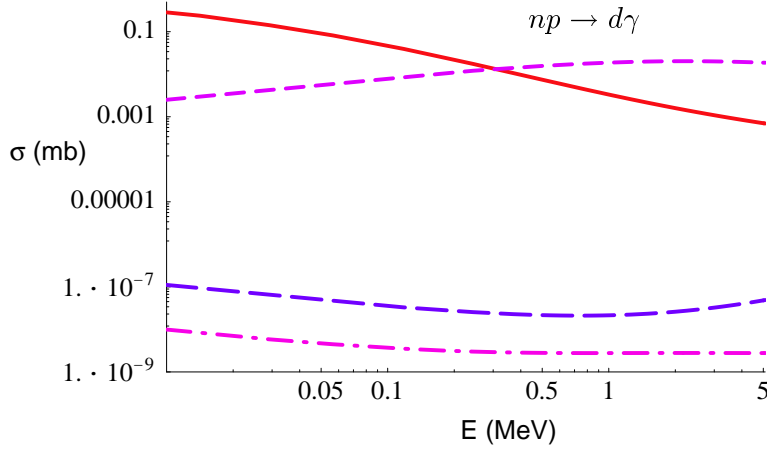


FIG. 1. $np \rightarrow d\gamma$ cross section σ (mb) for center of mass energy E (MeV), on a log-log plot. Solid curve: LO $M1_V$ transitions, dash: LO $E1_V$ transitions, long-dash: LO $M1_S$ transitions and dot-dash: LO $E2_S$ transitions.

$np \rightarrow d\gamma$ is measured to be $\sigma^{exp} = 334.2 \pm 0.5$ mb [17] and $M1_V$ transitions give the dominant contribution, Fig. 1. Thus at NLO, we fix L_{np} from this cold neutron capture rate:

$$\begin{aligned} \sigma^{(LO)} &\equiv \frac{4\pi\alpha(\gamma^2 + p^2)^3}{\gamma^3 M_{Np}^4} |\tilde{X}_{M1_V}^{(0)}|^2 \Big|_{p=p_0} \\ \sigma^{(NLO)} &\equiv \sigma^{exp} - \sigma^{(LO)} = \frac{4\pi\alpha(\gamma^2 + p^2)^3}{\gamma^3 M_{Np}^4} 2\text{Re}(\tilde{X}_{M1_V}^{(0)}(\tilde{X}_{M1_V}^{(1)})^*) \Big|_{p=p_0} \\ &\Rightarrow L_{np} = -9.039 \pm 0.027 \text{ fm}^2 . \end{aligned} \quad (3.17)$$

The $N^2\text{LO}$ terms also contribute to the cross section at momentum p_0 . Therefore, we impose the constraint [18]

$$\sigma^{(NNLO)} \equiv \frac{4\pi\alpha(\gamma^2 + p^2)^3}{\gamma^3 M_{Np}^4} \left[|\tilde{X}_{M1_V}^{(1)}|^2 + 2\text{Re}(\tilde{X}_{M1_V}^{(0)}(\tilde{X}_{M1_V}^{(2)})^*) \right] \Big|_{p=p_0} = 0 , \quad (3.18)$$

to reproduce the experimental cross section σ^{exp} . This determines the parameter

$$\tilde{L}_{np} = 4.957 \pm 0.011 \text{ fm}^2 . \quad (3.19)$$

The parameter L_{E1} , which contributes only to $E1_V$ transitions, cannot be determined reliably from this single data point since the $E1_V$ cross section is negligible at this low momentum p_0 . The error due to the experimental uncertainty in σ^{exp} is significant for energies $E \lesssim 0.25$ MeV. Above these energies the $E1_V$ cross section gives the dominant contribution and the error in $M1_V$ cross section can be ignored. The contribution of the four-nucleon-one-photon operator is found to be significant at low momentum $p_0 = 0.003443$ MeV. Neglecting this operator by setting $L_1^{M1_V} = 0$ at NLO underpredicts the experimental result σ^{exp} by 5%. This number is different from the one quoted in Ref. [8,15], where the $\rho_d\gamma$ expansion was used.

The parameter L_{E1} can be determined from photodisintegration of the deuteron. This cross section is related to the neutron capture cross section by [6,19]:

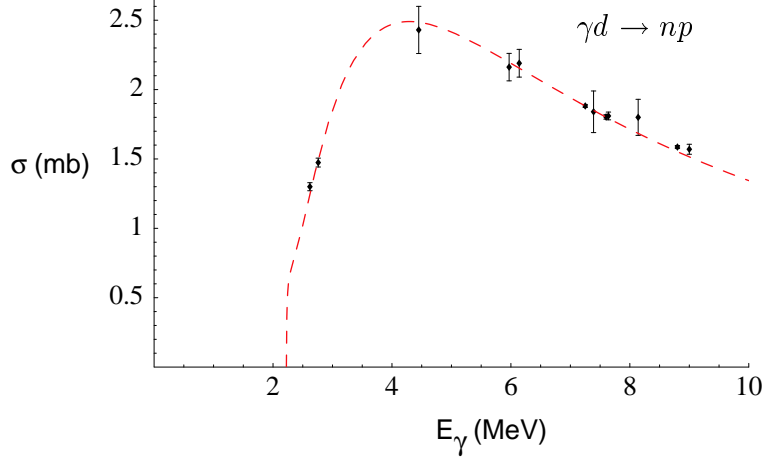


FIG. 2. Cross section in mb for $\gamma d \rightarrow np$ as a function of photon energy E_γ in MeV. The data is taken from Ref. [19], pages 78 and 79.

$$\sigma(\gamma d \rightarrow np) = \frac{2M_N}{3E_\gamma^2} \left[E_\gamma - B + \frac{B^2 - 6BE_\gamma + 4E_\gamma^2}{4M_N} \right] \sigma(np \rightarrow d\gamma), \quad (3.20)$$

where E_γ is the incident photon energy in the deuteron rest frame. Only the $E1_V$ transitions, on the right hand side of Eq. (3.20), receive relativistic corrections. In principle it is possible to determine all the three parameters L_{np} , \tilde{L}_{np} and L_{E1} from the deuteron breakup data. However, such a determination leads to significant uncertainty in the $M1_V$ cross section. This is because there are only two data points in the nucleon energy range sensitive to $M1_V$ transitions, $0.3 \text{ MeV} \lesssim E \approx E_\gamma - B \lesssim 0.5 \text{ MeV}$. We find that a χ^2 fit to data [19] in the photon energy range $2.6 \text{ MeV} < E_\gamma < 7.3 \text{ MeV}$ does not give a reliable constraint on the parameters L_{np} , \tilde{L}_{np} and L_{E1} . Constraining L_{np} and \tilde{L}_{np} from σ^{exp} as described above determines them more accurately. The other parameter L_{E1} is determined from a χ^2 fit to data [19] in the photon energy range $2.6 \text{ MeV} < E_\gamma < 7.3 \text{ MeV}$, where experimental errors in the total cross section from the $M1_V$ transition are negligible. This gives:

$$L_{E1} = -(5.3 \pm 3.6) \text{ fm}^3. \quad (3.21)$$

The error due to experimental uncertainty is $\lesssim 1\%$ over the range of $E \lesssim 5 \text{ MeV}$. This means that for nucleon energies relevant for BBN, $E \lesssim 0.2 \text{ MeV}$, the experimental uncertainty is significant compared to theoretical error, see Fig. 3. A few more high precision measurements in the incident photon energy range $2.5 \text{ MeV} \lesssim E_\gamma \lesssim 5 \text{ MeV}$ would provide important constraints on L_{E1} and determine the $np \rightarrow d\gamma$ cross section more accurately at energies relevant for big-bang nucleosynthesis.

The contribution from $N^4\text{LO}$ is found to be $\lesssim 3\%$ for incident photon energies $E_\gamma \lesssim 8 \text{ MeV}$ and is a small correction to the $N^3\text{LO}$ result [6]. This is better than the naive theoretical estimate for energies $E_\gamma > 4 \text{ MeV}$. This low energy theory, which is formally valid for energies $E_\gamma \lesssim 8 \text{ MeV}$, seems to reproduce data well above its range of validity, see Fig. 2.

Before discussing the results, it is important to check the self-consistency of our perturbative EFT calculation. The calculations were carried out under certain assumptions about the sizes of the couplings. The fact that the fitted couplings, Eqs. (3.17), (3.19) and (3.21), have sizes comparable to the theoretical estimates, Eqs. (3.13) and (3.7), suggests that the

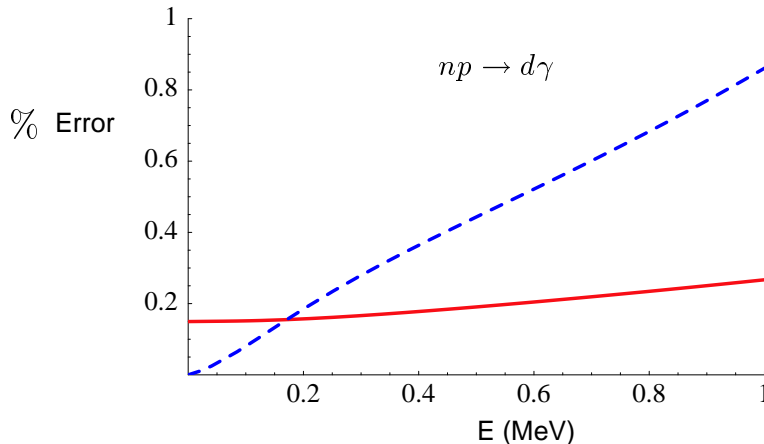


FIG. 3. Estimated theoretical error and experimental uncertainty in percentages versus nucleon center of mass energy E (MeV) for the $np \rightarrow d\gamma$ cross section. Solid curve: experimental uncertainty, dotted curve: estimated theoretical error.

perturbative expansion is under control to the order calculated. This allows us to make reliable error estimates.

IV. RESULTS

Table I shows the EFT $np \rightarrow d\gamma$ cross section for various nucleon center of mass energies, E . The corresponding values for the cross section from the on-line ENDF/B-VI database [3] are also shown in the last column. As explained earlier, an error of $(r_1 p^4/\gamma + r_0^3 p^6/\gamma^3)(1 + |1/(a^{exp}p)| + |1/(a^{exp}\gamma)|)$ with respect to LO was assigned to the $M1_V$ cross section and a conservative error of $\gamma(p^4 + p^2\gamma^2 + \gamma^4)/(6\pi\Lambda^5) - 5(Z_d - 1)\eta_d^2 + (Z_d - 1)(p^2 + \gamma^2)/M_N^2$ was assigned to the $E1_V$ cross section. The errors were added linearly to the total cross section and are found to be $\lesssim 1\%$ for $E \lesssim 1$ MeV. The EFT results are presented to only four significant digits, unless the theoretical errors enter earlier, in which case we keep up to the first digit where the errors contribute. Compared to the results in Ref. [6], these higher order EFT results are perturbatively closer to the ENDF/B-VI values. However, at some energies, e.g. 1×10^{-3} MeV, where the difference between the N³LO EFT result and ENDF value is much larger than the expected perturbative corrections, not surprisingly the discrepancy does not disappear by going to N⁴LO [6].

V. SUMMARY AND CONCLUSIONS

In finale, the big-bang nucleosynthesis prediction for primordial light element abundances uses the cross section for $np \rightarrow d\gamma$ as an input. A precise estimate of this cross section is thus critical for these predictions. The total cross section for radiative capture of neutrons on the proton $np \rightarrow d\gamma$ was calculated in EFT for center of mass energies $E \lesssim 1$ MeV. At the energies relevant for BBN, $0.02 \text{ MeV} \lesssim E \lesssim 0.2 \text{ MeV}$, the isovector electric transition $E1_V$ and the isovector magnetic transition $M1_V$ give the dominant contributions.

$\sigma(np \rightarrow d\gamma)$				
E (MeV)	$M1_V$ (mb)	$E1_V$ (mb)	$M1_V + E1_V$ (mb)	ENDF (mb) [3]
1.2625×10^{-8}	334.2 *	5.122×10^{-6}	334.2 *	332.0
$5. \times 10^{-4}$	1.667(0)	0.001019(3)	1.668(0)	1.660
$1. \times 10^{-3}$	1.170(0)	0.001441(5)	1.172(0)	1.193
$5. \times 10^{-3}$	0.4950(0)	0.00322(1)	0.4982(0)	0.496
$1. \times 10^{-2}$	0.3279(0)	0.00454(2)	0.3324(0)	0.324
$5. \times 10^{-2}$	0.09810(0)	0.00997(3)	0.1081(0)	0.108
0.100	0.04973(0)	0.01379(5)	0.06352(5)	0.0633
0.500	0.00787(3)	0.0263(1)	0.0341(2)	0.0345
1.00	0.0036(1)	0.0313(2)	0.0349(3)	0.0342

TABLE I. Cross section for $np \rightarrow d\gamma$ in mb for different center of mass energy E (MeV). For comparison, the values from the ENDF/B-VI on-line database are also shown. The first entry (*) is used for fitting a combination of parameters L_{np} 's, Eq. (3.17), (3.19). Another parameter L_{E1} was fitted to the deuteron photodisintegration $\gamma d \rightarrow np$ cross section, Eq. (3.21).

We calculated the $E1_V$ cross section to N⁴LO and the $M1_V$ cross section to N²LO. Up to N³LO, the $E1_V$ amplitude calculated in EFT is equivalent to the effective range theory result. Thus in principle, any calculation including potential models that reproduces nucleon-nucleon scattering data well will be able to describe the $E1_V$ amplitude to the accuracy of the N³LO calculation. However, the effective range theory result differs from the N⁴LO EFT result due to the absence of a four-nucleon-one-photon operator. This operator cannot be obtained from nucleon-nucleon scattering data alone. We determine this operator from the deuteron breakup $\gamma d \rightarrow np$ data with significant experimental uncertainty. Similarly, for the $M1_V$ transition there is a four-nucleon-one-photon operator at NLO that is not related to nucleon-nucleon scattering operators by gauge transformations. We determine this unknown operator from the cold neutron capture $np \rightarrow d\gamma$ rate and this operator contributes $\sim 2\%$ to the total cross section at $E = 0.5$ MeV. A few more precise measurements in the incident photon energy range $2.5 \text{ MeV} \lesssim E_\gamma \lesssim 5 \text{ MeV}$ would provide important constraints on the $M1_V$ and $E1_V$ transitions in the energies relevant for BBN. The sizes of the operators determined from data are consistent with their theoretical estimates. This verifies the theoretical assumptions about the perturbative expansion to the order of the calculation, which allows us to make reliable error estimates. For energies $E \lesssim 1$ MeV, the theoretical uncertainty in the total cross section is estimated to be $\lesssim 1\%$.

ACKNOWLEDGMENT

The author would like to thank Jiunn-Wei Chen, Daniel Phillips and Martin Savage for many helpful discussions. I would also like to thank Paulo Bedaque and Noam Shores for useful comments on the manuscript, and the other members of the EFT group at the University of Washington for valuable suggestions. This work is supported in part by the U.S. Dept. of Energy under Grant No. DE-FG0397ER4014.

REFERENCES

- [1] S. Burles, K.M. Nollet, J.N. Truran and M.S. Turner, *Phys. Rev. Lett.* **82**, 4176 (1999).
- [2] M.S. Smith, L.H. Kawano and R.A. Malaney, *Astrophys. J. Suppl. Ser.* **85**, 219 (1993).
- [3] ENDF/B-VI, Material 125, Revision 3, online database at the NNDC Online Data Service, <http://www.nndc.bnl.gov>.
- [4] G.M. Hale, *Private communication*.
- [5] W.A. Fowler, R.G. Caughlan, B.A. Zimmerman, *Annual Rev. of Astronomy and Astrophys.* **5**, 525 (1967).
- [6] J.W. Chen and M.J. Savage, nucl-th/9907042.
- [7] D.B. Kaplan, M.J. Savage and M.B. Wise, *Phys. Lett. B* **424**, 390 (1998), *Nucl. Phys. B* **534**, 329 (1998).
- [8] J.W. Chen, G. Rupak and M.J. Savage, *Nucl. Phys. A* **653**, 386 (1999).
- [9] D.R. Phillips, G. Rupak and M.J. Savage, nucl-th/9908054.
- [10] U. van Kolck, *Nucl. Phys. A* **645**, 273 (1999).
- [11] D.R. Phillips and T.D. Cohen, nucl-th/9906091.
- [12] V.G.J. Stoks, R.A.M. Klomp, C.P.F. Terheggen and J.J. de Swart, *Phys. Rev. C* **49**, 2950 (1994).
- [13] R.B. Wiringa, V.G.J. Stoks and R. Schiavilla, *Phys. Rev. C* **49**, 38 (1995).
- [14] D.O. Riska and G.E. Brown, *Phys. Lett. B* **38**, 193 (1972).
- [15] M.J. Savage, K.A. Scaldeferri and M.B. Wise, *Nucl. Phys. A* **652**, 273 (1999).
- [16] J.W. Chen, G. Rupak and M.J. Savage, nucl-th/9905002.
- [17] A.E. Cox, S.A.R. Wynchank and C.H. Collie, *Nucl. Phys.* **74**, 497 (1965).
- [18] G. Rupak and N. Shores, *Phys. Rev. C* **60**, 054004 (1999), nucl-th/9906077.
- [19] H. Arenhovel and M. Sanzone. *Photodisintegration of the Deuteron: A Review of Theory and Experiment*. ISBN 3-211-82276-3, Springer-Verlag, 1991.
- [20] J. Gegelia, nucl-th/9802038. T. Mehen and I. Stewart *Phys. Lett. B* **445**, 378 (1999).
- [21] J. Schwinger, Harvard lecture notes. Quoted by J. Blatt, *Phys. Rev.* **74**, 92 (1948). H.A. Bethe, *Phys. Rev.* **76**, 38 (1949).
- [22] J.J. de Swart, C.P.F. Terheggen and V.G.J. Stoks, nucl-th/9509032.
- [23] T.S. Park, K. Kubodera and M. Rho, *Phys. Rev. C* **58**, 637 (1998).
- [24] L. Koester and W. Nistler, *Z. Phys. A* **272**, 189 (1975).
- [25] V.G.J. Stoks, R.A.M. Klomp, M.C.M. Rentmeester and J.J. de Swart, *Phys. Rev. C* **48**, 792 (1993).
- [26] D.B. Kaplan, M.J. Savage and M.B. Wise, *Phys. Rev. C* **59**, 617 (1999).